Available online at www.sciencedirect.com
SCIENCE DIRECT®
Biochemical and Biophysical Research Communications 337 (2005) 670–676
BBRC
www.elsevier.com/locate/ybbrc

The N-terminal half of talin2 is sufficient for mouse development and survival

Nien-Tsu Chen, Su Hao Lo *

Center for Tissue Regeneration and Repair, Department of Orthopaedic Surgery and Cancer Center, University of California-Davis, Sacramento, CA 95817, USA

Received 10 September 2005
Available online 26 September 2005

Abstract

Using a talin2 gene-trapped embryonic stem cell clone, we have developed a talin2 mutant mouse line that expresses the N-terminal half (1–1295) of talin2 fused with β-galactosidase. The homozygous mutant mice appear to be normal and healthy. In the testis, talin2 expresses as a shorter form with a unique 30 residues at N-terminus linking to a common C-terminus from 1122 to 2453 of the long form. The resulting talin2 in the mutant testis only contains 204 residues of the wild-type testis talin2. However, it did not seem to affect the morphology of testis or reproduction of male mice. In fact, male and female mutant mice are fertile. Utilizing the expression of talin2(1–1295)/β-galactosidase fusion protein, we have examined the distribution of talin2 in tissues. In contrast to talin1, talin2 expression is more restricted in tissues and cell types.

Keywords: Talin2; Focal adhesions; Gene trap

Talin is a large focal adhesion component that interacts with multiple molecules, such as integrins [1–3], focal adhesion kinase (Fak) [4], vinculin [5], layilin [6], and actin [3]. Talin contains a head domain and a rod domain. The head domain (aa 1–433) of talin contains binding sites to β integrin (300–400), layilin (300–400), Fak (225–357), PIP kinase 1γ (300–400), and actin (196–400). The rod domain (483–2541) is responsible for the dimerization and contains an actin-binding domain (2345–2541), a second integrin binding site (1984–2113), and three vinculin-binding sites (607–633, 852–876, and 1944–1969). These binding activities allow talin to provide a structural connection between the integrin receptors and the actin cytoskeleton. In addition, talin regulates the "inside-out" integrin activation by binding to integrin tails leading to a higher affinity state [7].

Recent studies using laser tweezer microscopy have established a critical role of the interaction between talin and actin filament [8]. In the experiments, the force required to remove a bead coated with a cell-binding fragment of fibronectin from the lamellipodia of a normal fibroblast was measured. Such forces are significantly reduced in talin-null cells but are restored by re-expression of talin. However, re-expression of a talin mutant's lack of the C-terminal actin-binding site cannot restore the force [8]. These findings have demonstrated an important role of the talin–actin interaction in strengthening cell adhesion.

The critical role of talin in tissue development has been demonstrated by genetic studies using knockdown and knockout approaches. Reduction of talin expression in *Caenorhabditis elegans* caused severe defects in gonad formation because of aberrant distal tip cell migration and also disrupted oocyte maturation and gonad sheath cell structure [9]. Fly embryos deficient in talin exhibited failure in germ band retraction, muscle detachment, and wing blister [10]. Both *Drosophila* and *C. elegans* talin mutants have very similar phenotypes to those found in integrin

* Corresponding author. Fax: +1 916 734 5750.
E-mail address: shlo@ucdavis.edu (S.H. Lo).

0006-291X/$ - see front matter © 2005 Elsevier Inc. All rights reserved.
doi:10.1016/j.bbrc.2005.09.100

knockouts. Talin knockout in mice leads to embryonic lethality due to impaired cell migration at the gastrulation stage [11]. These studies have demonstrated that talin plays an essential role in tissue development.

A closely related member, talin2, has been identified [12]. Although talin2 is highly homologous to talin (or talin1), many of its potential binding activities and physiological roles remain to be established. Here, we reported the characterization of mice carrying a β-galactosidase insertion at talin2 gene, the distribution of talin2 in various tissues, and the identification of a testis splice form of talin2.

Materials and methods

Embryonic stem (ES) cells and mice. Talin2^{in1295} gene-trap SV129 ES cells (RRI434) were obtained from BayGenomics (UCSF) and injected into the C57BL/6 blastocysts. The resulting male chimeras were mated with C57BL/6 females, and the talin2^{in1295} line was subsequently maintained on a mixed C57BL/6:SV129 genetic background. Breeding was carried out under standard animal housing conditions in the UCD animal facility.

Genotyping was performed by polymerase chain reaction (PCR) assay. Mouse tail samples were lysed in lysis buffer (50 mM Tris–HCl, pH 7.4, 100 mM EDTA, pH 8.0, 400 mM NaCl, and 0.5% SDS) containing 1 mg/ml proteinase K at 55 °C for overnight. Primers specific for mouse talin2 and β-geo were: T2-F-gcccttccaggaggcccagagtgagc; T2-R-tatcacttgcatctg gtcttcttttg and βGeo-R-aattcagacggcaaacgactgtc. The PCR was performed at 94 °C for 5 min and followed by 30 cycles at 94 °C for 30 s, 65 °C for 30 s, and 72 °C for 2 min. Equal volume of each PCR product was analyzed by 1% agarose gel electrophoresis.

RNA preparation and Northern blot analysis. Total RNA was isolated from organs using Trizol (Invitrogen, Carlsbad, CA, USA) according to instruction of the manufacturer. For Northern blot analysis, an equal amount (15 μg) of RNAs from various tissues was separated on formaldehyde agarose gels and hybridized under high-stringency conditions in ExpressHyb hybridization solution (BD, Palo Alto, CA, USA) with ^{32}P-labelled probes at 68 °C for overnight. cDNA probes for hybridization were 747 and 658 bp corresponding to mouse talin2 3′ UTR (the stop codon and downstream) and β-Geo, respectively.

Western analysis. Fibroblasts were isolated from wild-type and talin2 mutant 14-day-old embryos as described [13]. Whole cell lysates (500 μg) were prepared as described [14] and immunoprecipitated with the anti-β-galactosidase (β-Gal, 1:500, ICN, Aurora OH, USA) at 4 °C for 1 h. The resulting immunoprecipitates and the whole cell lysates were analyzed by Western blotting using monoclonal antibodies at the following concentrations: anti-talin N-terminal (Talin-N, 1:1:000, Sigma, St. Louis, MO, USA), anti-talin C-terminal (Talin-C, 1:1000, Chemicon, Temecula, CA, USA), and anti-β-galactosidase (1:1000).

X-gal staining and histology. The brain, heart, eye, lung, kidney, and testis were dissected from talin2 mutant and wild-type mice. The organs were briefly fixed in fixation buffer (0.2% glutaraldehyde in PBS plus 2 mM $MgCl_2$, 5 mM EGTA, and 0.02% NP-40, pH 7.3) at 4 °C for 4 h. After three washes in PBS, samples were frozen and embedded in OCT (Sakura Finetek, Torrance CA, USA) compound. Frozen sections (8–10 μm) were prepared and stained for β-galactosidase activity. The sections were washed three times in washing buffer (PBS plus 2 mM $MgCl_2$, 5 mM EGTA, 0.02% NP-40, and 0.01% Na-deoxycholate, pH 7.3). The staining was carried out at 37 °C for 3–6 h in the washing buffer supplemented with 1 mg/ml X-gal, 5 mM potassium ferricyanide, and 5 mM potassium ferrocyanide. For histological analysis, tissues were fixed in 4% paraformaldehyde solution, processed, and embedded in paraffin. Sections were cut at 5-μm thickness, rehydrated, and stained with hematoxylin and eosin. Images were observed by Zeiss Axioplan2 microscope.

Results

Interruption of talin2 gene in mice

We have searched the available databases for mouse talin2 gene and two partial cDNA sequences (GenBank Accession Nos. AF467081 and BC059856) were identified. Together with the talin2 sequence from mouse chromosome 9 (XP_486227), we have assembled the mouse talin2 cDNA encoding 2453 amino acid residues, which shows 73% identity (85% similarity) with mouse talin1 (2541 amino acids, NM_011602) (Fig. 1).

By searching the BayGenomics database, we have found three gene-trapped embryonic stem (ES) cell lines with a disrupted talin2 gene [15]. The gene-trap construct which contained a strong splice acceptor was introduced into ES cells and resulted in an insertional mutation in the talin2 gene. Based on the available sequence information of the resulting mRNAs, we have selected the clone, RRI434, because its insertion site was more upstream than the other two clones (RRI055 and RRI102). The gene-trap construct was found inserted in the intron between exon 28 and exon 29 of talin2 and we named the allele talin2^{in1295} (for insertion mutant at amino acid residue 1295). This gene-trap insertion mutant was predicted to lead to the expression of talin2(1–1295)/β-galactosidase fusion proteins. Three primers (T2-F, T2-R, and βGeo-R) were designed to analyze the wild-type and the mutant alleles (Figs. 2A and B). The RRI434 ES cells were used to generate germ line chimeras and then heterozygous mutant mice. Crossing between heterozygous mice produced pups with expected Mendelian genotype ratio, indicating that this talin2 mutant did not lead to embryonic lethality. In addition, talin2 homozygous mutant mice were indistinguishable from heterozygous or wild-type mice. Both male and female homozygous mice were fertile. Histological sections including brain, heart, kidney, testis (Fig. 3), lung, liver, eye, and spleen (data not shown) were carefully examined and no sign of abnormality was found. The oldest mouse examined so far was 9 months old and again no defect was found.

Talin2 RNA expression in talin2 mutant mice

To confirm whether the gene-trap insertion has disrupted talin2 transcripts, we have analyzed the total RNAs isolated from wild-type and mutant tissues by Northern blotting. While strong signals around 9.5 and 7.5 kb were detected in wild-type brain and heart using a talin2-specific 3′ UTR probe, no band was detected in the brain, heart, and testis of mutant mice (Fig. 4). In addition, we have identified strong but shorter bands ~4.4 kb in wild-type testis and ~3.5 kb in wild-type and mutant kidneys. A 7.5-kb transcript was also observed in wild-type kidney. When the blot was re-probed for LacZ gene, signals were only detected in the samples from mutant mice. The detection of shorter talin2 transcripts was consistent with

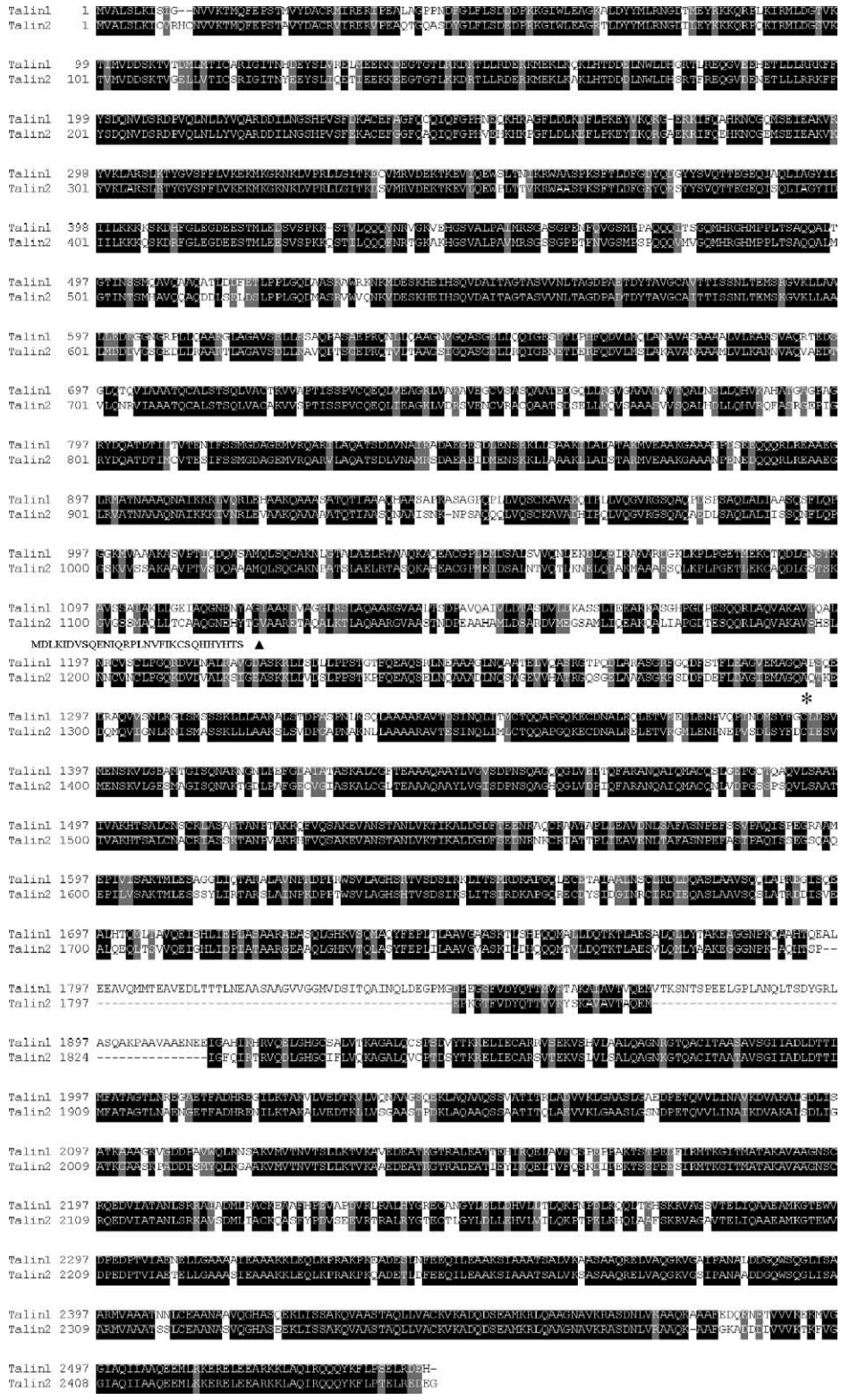

Fig. 1. Alignment of mouse talin1 and talin2 amino acid sequences. Amino acids surrounded in black and gray represent identity and similarity, respectively. Asterisk (*) indicates the site (aa 1295) fused to the β-galactosidase in the mutant; closed triangle (▲) shows the site (aa 1121) linked to the testis-specific 30 amino acids.

previous report [12] and may represent various alternative splice forms. By using the mouse talin2 sequence around the insertion site as a probe, we have searched the available databases. We found several cDNA sequences isolated from the testis (for example, GenBank Accession Nos. AK029828 and BB616043) that may represent the testis

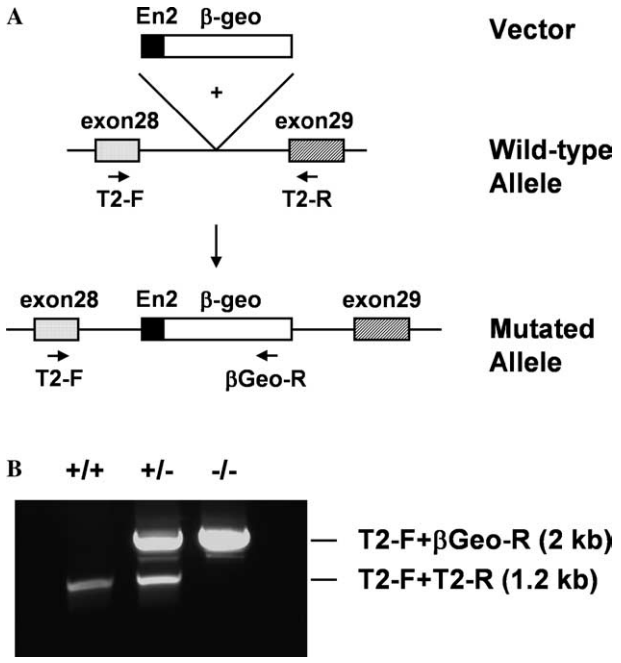

Fig. 2. Gene-trap mutagenesis of *talin2* gene locus. (A) Schematic representation of the partial genomic structure of the mouse talin2 gene before and after the gene-trap integration. T2-F, T2-R, and βGeo-R primers were designed to distinguish the wild-type allele from the mutated allele. (B) PCR analysis of DNA from siblings obtained in crosses of talin2 heterozygous parents. T2-F, T2-R, and βGeo-R primers were used to amplify a 1.2-kb fragment (wild-type allele) or a 2-kb fragment (mutated allele).

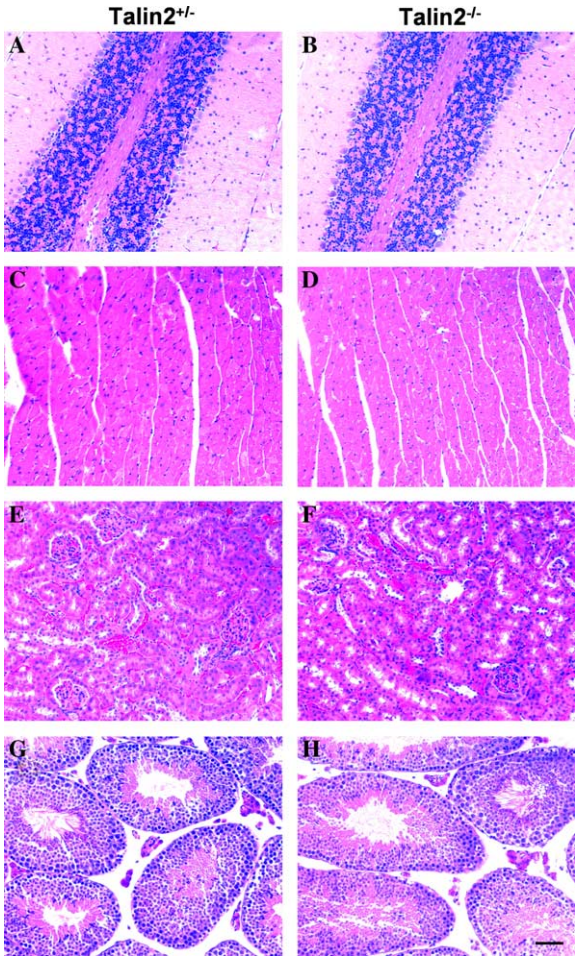

Fig. 3. Morphologies of brain, heart, kidney, and testis from adult wild-type and talin2 mutant mice. Paraffin sections of brain (A,B), heart (C,D), kidney (E,F), and testis (G,H) from 3-month-old talin2 heterozygous ($talin2^{+/-}$) and mutant ($talin2^{-/-}$) mice were stained with hematoxylin and eosin. Scale bar = 50 μm.

splice form of talin2. This splice form contains extra 251 base pairs encoding a unique 30 amino acid residues (M^{1}DLKIDVSQENIQRPLNVFIKCSQHHY HTS^{30}) at the N-terminus, followed by a sequence identical to the full-length talin2 residues from V^{1122}AARET to the end (Fig. 1). The resulting talin2 in the mutant testis only contained 204 residues of the wild-type testis talin2. However, no defect was found in the mutant testes and mutant mice were fertile. The transcriptional initiation site for the 3.5-kb transcript in the kidney is most likely located at further downstream to the insertion site. Therefore, the expression of this transcript was not affected by the gene-trap insertion and was detected in the mutant RNA sample (Fig. 4).

Talin2 protein expression in talin2 mutant cells

Based on the genomic and 5′ RACE analysis, this gene-trap insertion should lead to the expression of a chimeric protein with the N-terminal portion of talin2 (residue 1–1295) fused to the β-galactosidase. To test this, we have isolated fibroblasts from wild-type and mutant embryos for immunoprecipitation and Western blot analyses. Since talin2 is highly similar to talin1 (74% identity in human and 73% identity in mouse), there is no talin2-specific antibody available. In fact, most, if not all, talin1 antibodies cross-react with talin2. We used two talin antibodies, one against the N-terminal, the other against the C-terminal of talin for the assays. While both talin antibodies detected a single band in wild-type and mutant cell lysates, the talin-N antibodies appeared to be more sensitive and showed stronger signals (Fig. 5). In addition, there was a significant reduction in the mutant sample, presumably due to the ablation of talin2 and down-expression of talin1. When the cell lysates were first immunoprecipitated with anti-β-gal antibodies and then probed with various antibodies, only anti-talin-N, but not talin-C, antibodies could recognize the protein. These results demonstrated that talin2 was expressed as a talin2/β-galactosidase fusion protein in the mutant cells.

Talin2 tissue expression

To investigate the expression of talin2 in various tissues, we have taken advantage of this gene-trap mutant expressing talin2(1–1295)/β-galactosidase fusion protein under the endogenous talin2 promoter(s). Tissues from mice carrying the heterozygous/homozygous insertion allele were

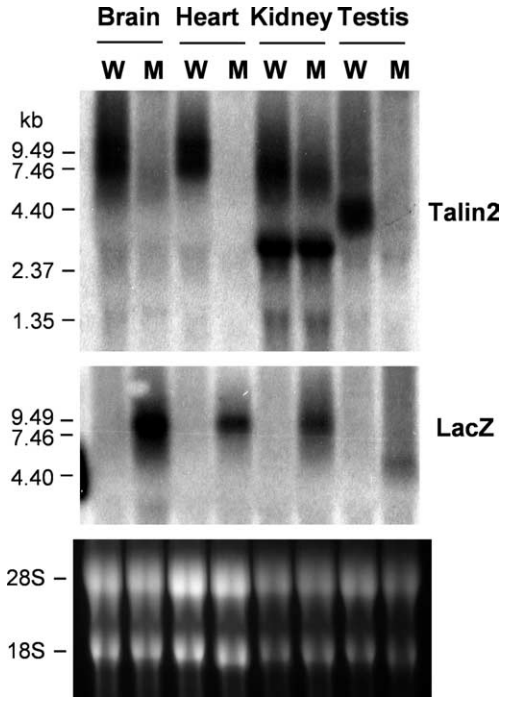

Fig. 4. Northern analysis of *talin2* gene and *lacZ* reporter gene expression in wild-type and talin2 mutant mice. Total RNAs from various tissues of wild-type (W) and talin2 mutant (M) mice were isolated. Equal amounts of RNAs (15 μg) from indicated tissues were separated on formaldehyde agarose gels and analyzed by Northern blot hybridization with talin2-specific probe (top panel). The same blot was stripped and re-probed with lacZ-specific (middle panel) probes. 28S and 18S ribosomal RNA were stained by ethidium bromide as a loading control (bottom panel).

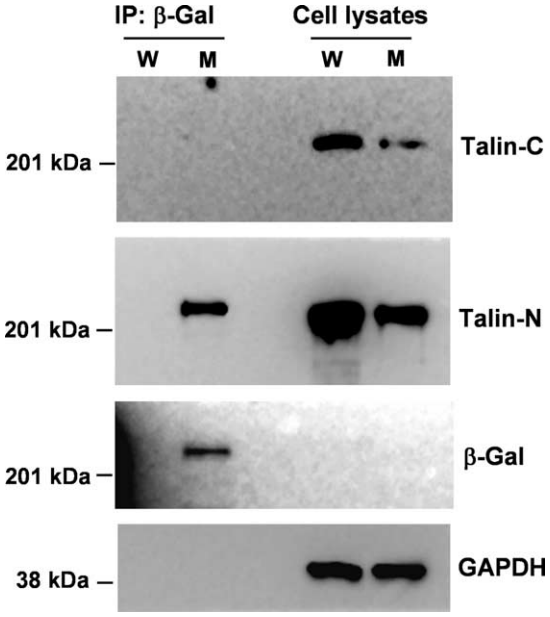

Fig. 5. Western blot analysis of talin proteins in embryonic fibroblasts from wild-type and talin2 mutant mice. Cell lysates (500 μg) from cultured embryonic fibroblasts of wild-type (W) and mutant (M) mice were subjected to immunoprecipitation (IP) with the anti-β-galactosidase (β-Gal) antibody. The resulting immunoprecipitates and the cell lysates (8 μg) were analyzed by Western blotting using antibodies recognizing the C-terminal of talin (Talin-C), the N-terminal of talin (Talin-N), and β-Gal. GAPDH was used as a protein loading and transferred control.

collected and sectioned for X-gal staining. As shown in Fig. 6, X-gal staining was detected in the dendrites of Purkinje cells in cerebellum (Fig. 6A); in myocardium of the heart (Fig. 6B); in choroidal stroma, pigmented epithelium, external limiting membrane, outer plexiform layer, and internal limiting membrane of the retina (Fig. 6C); in lung smooth muscle cells around bronchiole and blood vessels (Fig. 6D). The staining was very strong and concentrated in renal tubules (Fig. 6E) of papilla and medulla regions, but was dispersed in the cortex (Fig. 6F). In the testis, it was expressed in myoid cells and Leydig cells in 2-week-old mice (Fig. 6G) and also in spermatids in older mice (Fig. 6H). Tissues from wild-type mice did not show any X-gal staining (data not shown). Interestingly, most of the staining was concentrated on the basement membrane of the cells, suggesting that talin2, like talin1, was localized to the cell–matrix junctions and the N-terminal half of talin2 is sufficient for this localization.

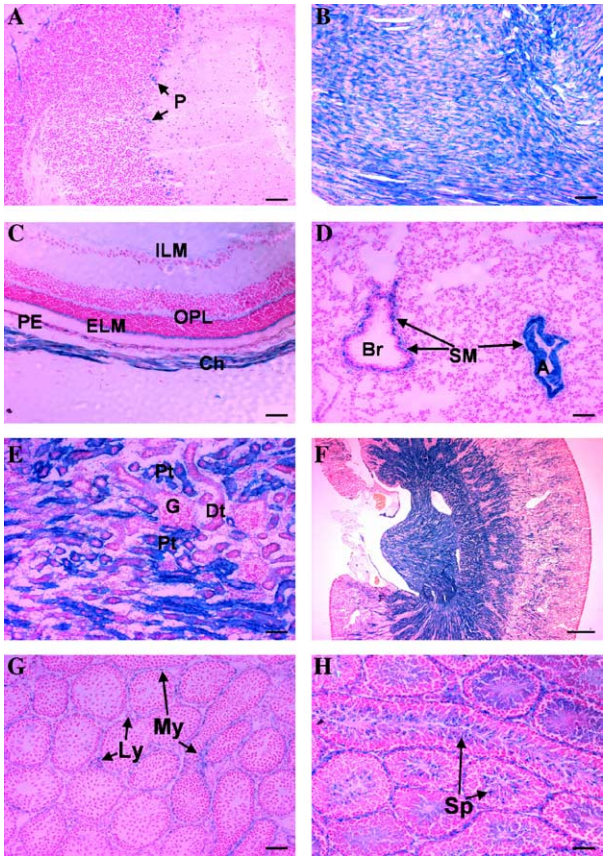

Fig. 6. X-gal staining of mice harboring the *lacZ* reporter gene. The expression of talin2(1–1295)/β-galactosidase fusion protein in brain (A), heart (B), eye (C), lung (D), kidney (E,F), and testis (G,H). Tissues from 2-week- (A–G) or 5-week- (H) old talin2 heterozygous mice were used for X-gal staining (blue stain). *Abbreviations:* P, Purkinje cells; PE, pigment epithelium; ELM, external limiting membrane; ILM, internal limiting membrane; OPL, outer plexiform layer; Ch, choroids; Br, bronchiole; SM, smooth muscle cells; A, artery; G, glomerulus; Pt, proximal tubule; Dt, distal tubule; Ly, Leydig cells; My, myoid cells; Sp, spermatids. Scale bar = 50 (A–E, G, and H) or 500 (F) μm. (For interpretation of the references to color in this figure legend, the reader is referred to the web version of this paper.)

Discussion

In addition to the mouse, the existence of a second talin gene was reported in humans [12] and *Dictyostelium* [16]. We also found partial sequences of talin2 in chimpanzee (*Pan troglodytes*), rat (*Rattus norvegicus*), cow (*Bos taurus*), dog (*Canis familiaris*), red jungle fowl (*Gallus gallus*), and zebrafish (*Danio rerio*) from EST databases. Their derived amino acid sequences are extremely conserved. For example, human (NM_015059), rat (XP_236367), and mouse are 95% identical. However, the mammalian talin2 is much less conserved with *Dictyostelium* talinA (24% identity) and talinB (25% identity).

Our total RNA Northern blot analysis has detected 9.5 and 7.5 kb talin2 transcripts in the brain and heart, 7.5 and 3.5 kb in the kidney, and a 4.4 kb in the testis (Fig. 4). In the other report using a poly(A) enriched mRNA blot [12], three talin2 transcripts around 10.5, 8.5, and 6.8 kb were detected in the brain and heart, 10.5, 8.5, 7.5, and 3.9 kb were identified in the kidney, and a 4.8-kb transcript was expressed in the testis. In general, our results are consistent with theirs, although the transcript sizes were slightly larger in their report. This may be due to the use of different markers. However, we neither detected the 6.8 kb band in the brain and heart nor the 10.5, 8.5 kb transcripts in the kidney in our total RNA blot. It is possible that the amounts of these transcripts were too low to be detected in our total RNA preparation. Alternatively, the 6.8-kb transcript in their study might not contain our 3′-UTR probe sequence. It is not clear why there are various talin2 transcripts. We found the testis splice form of talin2 that contains a unique 30 residues linked to a common C-terminal portion of talin2. This N-terminal sequence is derived from the extra 251 base pairs encoded by two additional exons (named 25a and 25b) between exon 25 and 26. The new start codon is located in exon 25b, which is 2.6 kb downstream of 25a. The distance between exon 25 and exon 25a is 2.9 kb, suggesting that this 2.9 kb fragment might contain a testis-specific promoter. If so, this promoter could be used in transgenic mice for specific expression in myoid and Leydig cells, and also in spermatids in older mice (Fig. 6G).

We have confirmed that this gene-trap insertion led to the expression of a chimeric protein with the N-terminal half of the talin2 fused to the β-galactosidase by immunoprecipitation and Western blotting approaches (Fig. 5). In addition, we have detected significantly weaker signals in mutant cell lysate samples using antibodies to talin. We initially attributed the weaker talin signals in mutant cell lysate samples to lack of the C-terminal half of talin2. However, the N-terminal portion of talin2 was still expressed in the mutant and we would predict that an equal or even higher (due to talin1 compensation) amount of talin would be found in the mutant samples using the antibodies against the N-terminus of talin. Therefore, the down-regulation of talin1 also contributed to the weaker signals. In fact, it might be the main reason for the significant reduction of talin signals, because the amount of talin2(1–1295)/β-galactosidase fusion protein was very low and was not readily detectable unless was concentrated by immunoprecipitation (Fig. 5) . Why and how talin1 was down-regulated in the mutant cells is not clear. One possibility is that talin1 proteins form homodimers, as well as a small population of heterodimers with talin2, and the heterodimers may stabilize talin1 homodimers in normal cells. Talin2(1–1295)/β-galactosidase fusion proteins could not form heterodimers and stabilize talin1 dimers, leading to the lower amount of total talin1 in mutant cells.

Previous studies on deletion of talin1 gene in mice have demonstrated its critical role in embryonic development [9]. Many other reports have indicated that talin plays a very important role in the structure and signaling of focal adhesions [17]. Since talin1 and talin2 are highly conserved and most of the antibodies used for previous analyses were not able to distinguish one from the other, some of the proposed functions for talin might be contributed and/or shared by talin2. For example, talin2 is shown to bind to PIP kinase 1γ [18] and actin [19]. Therefore, it somehow surprised us that no significant abnormality was found in this talin2 mutant mouse line. Talin2 is like talin1 a large protein with 2453 amino acid residues. In this case, we would expect that lack of the C-terminal half of talin2 and in some splice forms the majority of protein (for example, testis form) would impair the dimerization, the second integrin binding, vinculin-binding, and actin-binding activities located at the deleted C-terminus. In addition, the remaining N-terminal half might function as a dominant negative fragment. In fact, we also found down-regulation of talin1 in mutant cells. However, the mutant did not appear to affect embryogenesis, tissue development and function, and fertility of these mice. There are several possibilities, including (1) talin1 alone is sufficient for talin's function, (2) the N-terminus 1–1295 fragment has account for all talin2's function, and (3) some minor defects were not identified and/or defects in repair or regeneration process will not reveal without insult. The true answer probably will not be revealed until a completed talin2 knockout mouse is available.

Acknowledgments

We thank the BayGenomics for providing the gene-trapped ES clone. This study is supported in part by Shriner's Children Hospital grant (S.H.L.).

References

[1] A. Horwitz, K. Duggan, C. Buck, M.C. Beckerle, K. Burridge, Interaction of plasma membrane fibronectin receptor with talin—a transmembrane linkage, Nature 320 (1986) 531–533.
[2] B. Xing, A. Jedsadayanmata, S.C. Lam, Localization of an integrin binding site to the C terminus of talin, J. Biol. Chem. 276 (2001) 44373–44378.
[3] L. Hemmings, D.J. Rees, V. Ohanian, S.J. Bolton, A.P. Gilmore, B. Patel, H. Priddle, J.E. Trevithick, R.O. Hynes, D.R. Critchley,

Talin contains three actin-binding sites each of which is adjacent to a vinculin-binding site, J. Cell Sci. 109 (Pt. 11) (1996) 2715–2726.
[4] H.C. Chen, P.A. Appeddu, J.T. Parsons, J.D. Hildebrand, M.D. Schaller, J.L. Guan, Interaction of focal adhesion kinase with cytoskeletal protein talin, J. Biol. Chem. 270 (1995) 16995–16999.
[5] M.D. Bass, B. Patel, I.G. Barsukov, I.J. Fillingham, R. Mason, B.J. Smith, C.R. Bagshaw, D.R. Critchley, Further characterization of the interaction between the cytoskeletal proteins talin and vinculin, Biochem. J. 362 (2002) 761–768.
[6] M.L. Borowsky, R.O. Hynes, Layilin, a novel talin-binding transmembrane protein homologous with C-type lectins, is localized in membrane ruffles, J. Cell Biol. 143 (1998) 429–442.
[7] D.A. Calderwood, Integrin activation, J. Cell Sci. 117 (2004) 657–666.
[8] G. Jiang, G. Giannone, D.R. Critchley, E. Fukumoto, M.P. Sheetz, Two-piconewton slip bond between fibronectin and the cytoskeleton depends on talin, Nature 424 (2003) 334–337.
[9] E.J. Cram, S.G. Clark, J.E. Schwarzbauer, Talin loss-of-function uncovers roles in cell contractility and migration in *C. elegans*, J. Cell Sci. 116 (2003) 3871–3878.
[10] N.H. Brown, S.L. Gregory, W.L. Rickoll, L.I. Fessler, M. Prout, R.A. White, J.W. Fristrom, Talin is essential for integrin function in Drosophila, Dev. Cell 3 (2002) 569–579.
[11] S.J. Monkley, X.H. Zhou, S.J. Kinston, S.M. Giblett, L. Hemmings, H. Priddle, J.E. Brown, C.A. Pritchard, D.R. Critchley, R. Fassler, Disruption of the talin gene arrests mouse development at the gastrulation stage, Dev. Dyn. 219 (2000) 560–574.
[12] S.J. Monkley, C.A. Pritchard, D.R. Critchley, Analysis of the mammalian talin2 gene TLN2, Biochem. Biophys. Res. Commun. 286 (2001) 880–885.
[13] A. Ishii, S.H. Lo, A role of tensin in skeletal-muscle regeneration, Biochem. J. 356 (2001) 737–745.
[14] H. Chen, A. Ishii, W.K. Wong, L.B. Chen, S.H. Lo, Molecular characterization of human tensin, Biochem. J. 351 (Pt. 2) (2000) 403–411.
[15] W.C. Skarnes, Gene trapping methods for the identification and functional analysis of cell surface proteins in mice, Methods Enzymol. 328 (2000) 592–615.
[16] M. Kreitmeier, G. Gerisch, C. Heizer, A. Muller-Taubenberger, A talin homologue of *Dictyostelium* rapidly assembles at the leading edge of cells in response to chemoattractant, J. Cell Biol. 129 (1995) 179–188.
[17] A. Nayal, D.J. Webb, A.F. Horwitz, Talin: an emerging focal point of adhesion dynamics, Curr. Opin. Cell Biol. 16 (2004) 94–98.
[18] G. Di Paolo, L. Pellegrini, K. Letinic, G. Cestra, R. Zoncu, S. Voronov, S. Chang, J. Guo, M.R. Wenk, P. De Camilli, Recruitment and regulation of phosphatidylinositol phosphate kinase type 1 gamma by the FERM domain of talin, Nature 420 (2002) 85–89.
[19] M.A. Senetar, S.J. Foster, R.O. McCann, Intrasteric inhibition mediates the interaction of the I/LWEQ module proteins Talin1, Talin2, Hip1, and Hip12 with actin, Biochemistry 43 (2004) 15418–15428.